

The role of the radical-complex mechanism in the ozone recombination/dissociation reaction

Klaus Luther, Kawon Oum and Jürgen Troe*

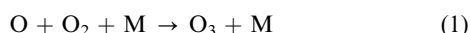
Institut für Physikalische Chemie, Universität Göttingen, Tammannstrasse 6, D-37077 Göttingen, Germany. E-mail: shoff@gwdg.de; Fax: +49 551 393121; Tel: +49 551 393150

*Received 23rd March 2005, Accepted 27th May 2005
First published as an Advance Article on the web 10th June 2005*

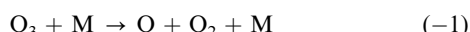
The data bases for low-pressure rate coefficients of the dissociation of O₃ and the reverse recombination of O with O₂ in the bath gases M = He, Ar, N₂, CO₂ and SF₆ are carefully analyzed. At very high temperatures, the rate constants have to correspond solely to the energy transfer (ET) mechanism. On condition that this holds for Ar and N₂ near 800 K, average energies transferred per collision of $-\langle\Delta E\rangle/hc = 18$ and 25 cm^{-1} are derived, respectively. Assuming an only weak temperature dependence of $\langle\Delta E\rangle$ as known in similar systems, rate coefficients for the ET-mechanism are extrapolated to lower temperatures and compared with the experiments. The difference between measured and extrapolated rate coefficients is attributed to the radical complex (RC) mechanism. The derived rate coefficients for the RC-mechanism are rationalized in terms of equilibrium constants for equilibria of van der Waals complexes of O (or O₂) with the bath gases and with rate coefficients for oxygen abstraction from these complexes. The latter are of similar magnitude as rate coefficients for oxygen isotope exchange which provides support for the present interpretation of the reaction in terms of a superposition of RC- and ET-mechanisms. We obtained rate coefficients for the ET-mechanism of $k_{\text{rec},0}^{\text{ET}}/[\text{Ar}] = 2.3 \times 10^{-34} (T/300)^{-1.5}$ and $k_{\text{rec},0}^{\text{ET}}/[\text{N}_2] = 3.5 \times 10^{-34} (T/300)^{-1.5}\text{ cm}^6\text{ molecule}^{-2}\text{ s}^{-1}$ and rate coefficients for the RC-mechanism of $k_{\text{rec},0}^{\text{RC}}/[\text{Ar}] = 1.7 \times 10^{-34} (T/300)^{-3.2}$ and $k_{\text{rec},0}^{\text{RC}}/[\text{N}_2] = 2.5 \times 10^{-34} (T/300)^{-3.3}\text{ cm}^6\text{ molecule}^{-2}\text{ s}^{-1}$. The data bases for M = He, CO₂ and SF₆ are less complete and only approximate separations of RC- and ET-mechanism were possible. The consequences of the present analysis for an analysis of isotope effects in ozone recombination are emphasized.

1 Introduction

The thermal recombination reaction

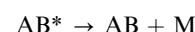
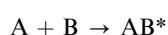


and the reverse thermal dissociation of ozone

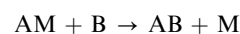
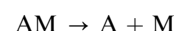


have been studied extensively in experiments covering the temperature range 80–3000 K, the pressure range 10^{-4} – 10^3 bar, and a large number of bath gases M. Experiments up to 1973 have been summarized in ref. 1. Later recombination experiments were discussed in CODATA/IUPAC evaluations like refs. 2–4 or in NASA evaluations like ref. 5. There have been only few later dissociation studies such as summarized in the present work. Combining recombination and dissociation studies by the help of the equilibrium constant,⁶ a large body of data exist for the recombination/dissociation reaction (1) and (–1) which wait for a quantitative analysis.

Applying standard unimolecular rate theory to the data available in 1979, the treatment given in refs. 7–9 did not reveal anything unusual, except the conclusion that collisional energy transfer was fairly inefficient. The picture changed when recombination experiments were extended down to 80 K in refs. 10 and 11 and up to pressures of 10^3 bar in ref. 11. The pressure dependence did not show the falloff behaviour of a typical unimolecular reaction and the temperature dependence below 300 K was much stronger than expected for a unimolecular reaction governed by the energy transfer (ET) mechanism, *i.e.* a mechanism following the scheme



The situation in ref. 11 was rationalized by suggesting that the reaction at low temperatures was dominated by the radical-complex (RC) or Chaperon mechanism, *i.e.* a mechanism following the scheme



and that only at high temperatures the ET-mechanism took over. The rates for the two mechanisms were estimated at least semiquantitatively, providing a rational interpretation of the experimental observations. The transition between the RC- and the ET-mechanism was suggested to happen near 200 K for M = He and near 400 K for M = Ar and N₂.

Since 1990 attention has shifted away from the absolute rates for reactions (1) and (–1) towards an interpretation of unusual isotope effects in the recombination reaction (1) such as they are of great interest for atmospheric chemistry, see *e.g.* refs. 12–14. Theoretical attempts to explain the observed isotope effects have been numerous, see *e.g.* refs. 15–18; however, mostly the ET-mechanism was employed. The ET-mechanism in ref. 17 was also used to reproduce absolute values of the recombination rate coefficients between 130–300 K. However, much larger collision efficiencies for energy transfer had to be employed than suggested in ref. 11. Looking only at the limited temperature range considered in ref. 17 does not appear sufficient to solve the problem. In any case, one cannot expect

to explain the isotope effects without understanding the whole body of available dissociation/recombination data. The question of an adequate interpretation of isotope effects and rate data for reactions (1) and (−1), therefore, to the present authors remains open. Both isotope effects and ozone recombination rates are of large importance for atmospheric chemistry. They are interconnected and have to be analyzed together. Other theoretical studies of the recombination reaction in terms of the energy transfer mechanism¹⁹ apparently were too simplified to explain the experimental rates. A single theoretical attempt to explain the recombination rates in terms of the RC-mechanism²⁰ missed the experimental rates by one order of magnitude.

The reason why we come back 15 years after ref. 11 to an interpretation of ozone dissociation/recombination rates is twofold. Our knowledge on the ozone potential energy surface has been improved very much (see refs. 21–23). In addition, we have collected experience with the analysis of the radical-complex mechanism in other reaction systems, see e.g. ref. 24. Furthermore, theoretical work with the new *ab initio* potential on oxygen isotope exchange in the reaction $\text{O} + \text{O}_2 \rightarrow \text{O}_2 + \text{O}$,²⁵ on collisional energy transfer of highly vibrationally excited ozone²⁶ as well as on the RC-mechanism in ozone recombination²⁷ seems to fall in line with our analysis from ref. 11. It, therefore, appears advisable to reanalyze more carefully the available data base of dissociation/recombination rate coefficients on the basis of our improved knowledge of molecular parameters.

At this stage, we focus attention on the low-pressure range only because that range is difficult enough to understand. Our strategy is as follows: we first consider measurements at the highest available temperatures and assume that here the reaction is dominated by the ET-mechanism. Employing state-of-the-art unimolecular rate theory to these data, we derive the average energy $\langle \Delta E \rangle$ transferred per collision. This quantity then is the only parameter from the ET-mechanism which needs to be fitted empirically because theoretical determinations are not yet sufficiently reliable for cases like O_3 . In agreement with other experimental systems governed by the ET-mechanism, we assume that $\langle \Delta E \rangle$ has only a weak temperature dependence. This allows one to extrapolate the rate coefficients for the ET-mechanism towards lower temperatures. A comparison with the experimental rate coefficients at lower temperatures then leads to the RC-contribution of the rate. The derived rate coefficients for the RC-mechanism finally are analyzed in terms of O-M and $\text{O}_2\text{-M}$ radical-complex equilibrium constants and rate coefficients for the reactions $\text{OM} + \text{O}_2 \rightarrow \text{O}_3 + \text{M}$ or $\text{O}_2\text{M} + \text{O} \rightarrow \text{O}_3 + \text{M}$. These results are compared with analogous quantities of other RC-systems like those investigated in ref. 24. The consequences of our analysis for an understanding of the pressure dependence and of isotope effects finally are indicated.

2 Modelling of the ET-mechanism

The ET-mechanism of reaction (1) can be characterized symbolically by the steps



For dissociation, there is the additional step



while step (2) is absent. In the present work we only consider the low-pressure range of the reaction (termolecular for recombination, bimolecular for dissociation). In this case, the limiting low-pressure rate coefficients (pseudo-second-order for

recombination and pseudo-first-order for dissociation) are written symbolically as

$$k_{\text{rec},0} = k_3[\text{M}](k_2/k_{-2}) \quad (4)$$

and

$$k_{\text{diss},0} = k_{-3}[\text{M}] = k_3[\text{M}](\text{[O}_3^*]/\text{[O}_3])_{\text{eq}} \quad (5)$$

while the equilibrium constant is given by

$$K_{\text{eq}} = k_{\text{rec},0}/k_{\text{diss},0} = k_2k_3/k_{-2}k_{-3}. \quad (6)$$

By analytically solving the steady-state master equation of the dissociation²⁸ and the recombination²⁹ reaction, eqn. (5) takes the form

$$k_{\text{diss},0} = Z[\text{M}]\beta_c \sum_{J=0}^{\infty} (2J+1) \int_{E_0(J)}^{\infty} f(E,J) dE \quad (7)$$

with the overall collision frequency Z for energy transfer, the collision efficiency β_c , the threshold energy $E_0(J)$ as a function of angular momentum (quantum number J) and the equilibrium population $f(E,J)$ as a function of J and the energy E . The sum and the integral $\sum \int$ in eqn. (7) correspond to $(\text{[O}_3^*]/\text{[O}_3])_{\text{eq}}$ in eqn. (5). The solution of the master equation allows one to relate β_c with the average energy $\langle \Delta E \rangle$ transferred per collision, for which

$$\beta_c/(1 - \beta_c^{1/2}) \approx -\langle \Delta E \rangle / F_E kT \quad (8)$$

was derived in ref. 28. For the sake of transparency, the sum and the integral $\sum \int$ were expressed in factorized form by

$$k_{\text{diss},0} = Z[\text{M}]\beta_c(\rho_{\text{vib},h}(E_0)kT/Q_{\text{vib}})F_E F_{\text{anh}} F_{\text{rot}} \exp(-E_0/kT) \quad (9)$$

in refs. 8 and 9. In this expression one has the harmonic vibrational density of states $\rho_{\text{vib},h}(E_0)$ and the vibrational partition function Q_{vib} , while the factors F_E , F_{anh} and F_{rot} account for the energy dependence of $\rho_{\text{vib},h}(E)$, for vibrational anharmonicity, and for rotational effects including the influence of $E_0(J)$, respectively. With the equilibrium constant

$$K_{\text{eq}} = Q(\text{O}_3)/[Q(\text{O})Q(\text{O}_2)\exp(-E_0/kT)], \quad (10)$$

eqn. (9) leads to

$$k_{\text{rec},0} = Z[\text{M}]\beta_c \left(\frac{\rho_{\text{vib},h}(E_0)kT}{Q_{\text{vib}}(\text{O}_3)} \right) F_E F_{\text{anh}} F_{\text{rot}} \left(\frac{Q(\text{O}_3)}{Q(\text{O})Q(\text{O}_2)} \right) \quad (11)$$

where the partition functions Q contain translational, rotational, vibrational and electronic contributions.

The various factors in eqns. (10) and (11) in refs. 8, 9 and 11 have been calculated on the basis of the then available knowledge of the molecular parameters. By comparison with the experiments finally β_c and, through eqn. (8), $\langle \Delta E \rangle$ were fitted. E.g., $-\langle \Delta E \rangle/hc = (20 \pm 10) \text{ cm}^{-1}$ in ref. 11 were derived for $\text{M} = \text{He}$, Ar and N_2 near 800 K. These values were found to be in fair agreement with the results from classical trajectory calculations of refs. 30 and 31. The analysis from ref. 17 gave much larger values, being around 200 cm^{-1} for deactivating collisions which would correspond⁸ to about $-\langle \Delta E \rangle/hc \approx 100 \text{ cm}^{-1}$ at 300 K. The present analysis disputes such interpretation.

Because the characterization of the ET-contribution to $k_{\text{rec},0}$ is a central element of our interpretation, we repeat the calculation of the factors in eqns. (10) and (11) on the basis of the improved molecular parameters available today. The calculation of the various factors is elaborated in the Appendix. The resulting rate coefficients even over the large temperature range 80–3000 K can be well approximated by a $k_{\text{rec},0} \propto T^{-n}$ dependence with a temperature independent exponent n . $\langle \Delta E \rangle$ is fitted by the experimental values at 800 K and then used without further change.

Table 1 Low-pressure rate coefficients $k_{\text{rec},0}^{\text{ET}}$ for the energy transfer mechanism and equilibrium constants K_{eq} (T in K, $k_{\text{rec},0}^{\text{ET}}/[\text{M}]$ and strong collision rate coefficients $k_{\text{rec},0}^{\text{ET,SC}}/[\text{M}]$ in $\text{cm}^6 \text{ molecule}^{-2} \text{ s}^{-1}$, K_{eq} in $\text{cm}^3 \text{ molecule}^{-1}$)

T/K	80	100	200	300	400	500	800	1000	1600
$k_{\text{rec},0}^{\text{ET}}/[\text{Ar}]$	1.7×10^{-33}	1.2×10^{-33}	4.3×10^{-34}	2.3×10^{-34}	1.5×10^{-34}	1.1×10^{-34}	5.1×10^{-35}	3.6×10^{-35}	1.6×10^{-35}
$k_{\text{rec},0}^{\text{ET,SC}}/[\text{Ar}]$	9.3×10^{-33}	8.0×10^{-33}	4.9×10^{-33}	3.7×10^{-33}	3.1×10^{-33}	2.8×10^{-33}	2.1×10^{-33}	1.8×10^{-33}	1.3×10^{-33}
$k_{\text{rec},0}^{\text{ET}}/[\text{N}_2]$	2.4×10^{-33}	1.8×10^{-33}	6.5×10^{-34}	3.5×10^{-34}	2.3×10^{-34}	1.6×10^{-34}	8.0×10^{-35}	5.6×10^{-35}	2.5×10^{-35}
$k_{\text{rec},0}^{\text{ET,SC}}/[\text{N}_2]$	1.1×10^{-32}	9.1×10^{-33}	5.6×10^{-33}	4.3×10^{-33}	3.6×10^{-33}	3.2×10^{-33}	2.4×10^{-33}	2.1×10^{-33}	1.5×10^{-33}
K_{eq}	—	—	—	—	9.6×10^{-13}	1.8×10^{-15}	1.6×10^{-19}	7.7×10^{-21}	8.8×10^{-23}

The assumption of a nearly temperature independent $\langle \Delta E \rangle$ appears justified, if one looks at related dissociation/recombination reactions being evaluated by the same procedure. *E.g.*, the well studied recombination $\text{H} + \text{O}_2 + \text{M} \rightarrow \text{HO}_2 + \text{M}$ in the bath gases $\text{M} = \text{Ar}$ and N_2 in ref. 32 over the temperature range 220–1500 K was analyzed in the same way as the present treatment; values of $-\langle \Delta E \rangle/hc = 21 (T/300)^{+0.1} \text{ cm}^{-1}$ for $\text{M} = \text{Ar}$ and of $60 (T/300)^{-0.2} \text{ cm}^{-1}$ for $\text{M} = \text{N}_2$ were derived. Likewise, the evaluation of the reaction $\text{H} + \text{CH}_3 + \text{M} \rightarrow \text{CH}_4 + \text{M}$ over the temperature range 1000–5000 K with $\text{M} = \text{Ar}$ ³³ led to $-\langle \Delta E \rangle/hc = 50 (T/300)^{0 \pm 0.3} \text{ cm}^{-1}$ while, for $\text{M} = \text{He}$,³⁴ $-\langle \Delta E \rangle/hc \approx 20 (T/300)^{1 \pm 0.5} \text{ cm}^{-1}$ was found over the range 300–1000 K. A look at other reaction systems in ref. 33 confirms that $\langle \Delta E \rangle$ in the present type of analysis either is practically temperature independent or at most has a small positive temperature coefficient up to about T^1 for $\text{M} = \text{He}$. It appears important to emphasize that $\langle \Delta E \rangle$ is not expected to have a large negative temperature coefficient, see below.

In this work we analyze experimental data for reactions (1) and (–1) in the bath gases $\text{M} = \text{He}, \text{Ar}, \text{N}_2, \text{CO}_2$ and SF_6 . In the discussed way we fit $\langle \Delta E \rangle$ to the experimental results near 800 K, assuming that $k_{\text{rec},0}$ here is dominated by the ET-mechanism. In the next section the individual cases are considered in more detail. The analysis of the data is based on $k_{\text{rec},0}/[\text{M}] = (12, 5.1, 8.0, 36, 61) \times 10^{-35} \text{ cm}^3 \text{ molecule}^{-1} \text{ s}^{-1}$ at 800 K, see below, which leads to the values $-\langle \Delta E \rangle/hc = (18, 18, 25, 150, 280) \text{ cm}^{-1}$ at 300 K for the bath gases $\text{M} = \text{He}, \text{Ar}, \text{N}_2, \text{CO}_2$ and SF_6 , respectively. The values of $\langle \Delta E \rangle$ are assumed to be nearly temperature independent, except for $\text{M} = \text{He}$ where $\langle \Delta E \rangle \propto T^{0.5}$ follows from the data, see below. The corresponding temperature-dependent values of the rate coefficients from the ET-mechanism in Table 1 are compared with the strong collision rate coefficients $k_{\text{rec},0}^{\text{ET,SC}}/[\text{M}]$, *i.e.* the calculated values from eqn. (11) with β_c from eqn. (8).

3 Experimental determination of the contribution from the RC-mechanism

In the following the experimental results are compared with the rate coefficients from the ET-mechanism such as determined in section 2 and fitted to experimental data near 800 K. Because this comparison provides the empirical justification for our conclusions on the RC-mechanism, particular care had to be taken to obtain the best available experimental data base. We, therefore, have gone back to the individual experimental studies and, in part, re-evaluated the data with improved knowledge^{1–5} on the rates of reference reactions.

The most complete data base is available for $\text{M} = \text{Ar}$ where the experiments from refs. 7, 10, 11, 35–48 cover the temperature range 80–3000 K which is probably the largest range which would be accessible experimentally. (The experiments from ref. 43 in the range 1100–3000 K become increasingly scattered at temperatures above 1500 K and in shock waves using more than 1% O_3 in Ar. We, therefore, discard experimental data above 1500 K and using higher ozone concentrations; these data were included in ref. 11.) Fig. 1 shows the data. One notices a large negative temperature coefficient. One also observes a slight change of the temperature coefficient

from low to high temperatures. The experimental $k_{\text{rec},0}$ markedly differs from the ET-calculations which we denote by $k_{\text{rec},0}^{\text{ET}}$, see Table 1. We attribute this behaviour to the contribution of the RC-mechanism to $k_{\text{rec},0}$ which we determine from

$$k_{\text{rec},0}^{\text{RC}} = k_{\text{rec},0} - k_{\text{rec},0}^{\text{ET}} \quad (12)$$

For $\text{M} = \text{Ar}$, in this way we obtain

$$k_{\text{rec},0}^{\text{RC}}/[\text{Ar}] = 1.7 \times 10^{-34} (T/300)^{-3.2} \text{ cm}^6 \text{ molecule}^{-2} \text{ s}^{-1} \quad (13)$$

while

$$k_{\text{rec},0}^{\text{ET}}/[\text{Ar}] = 2.3 \times 10^{-34} (T/300)^{-1.5} \text{ cm}^6 \text{ molecule}^{-2} \text{ s}^{-1}. \quad (14)$$

The interpretation of the experimental rate coefficients $k_{\text{rec},0}$ by the ET-mechanism, in terms of eqns. (8) and (11) alone, would require a markedly negative temperature coefficient of $\langle \Delta E \rangle$. In order to reproduce the measured $k_{\text{rec},0}$ one would have to use $-\langle \Delta E \rangle/hc \approx 50 (T/300)^{-1} \text{ cm}^{-1}$. Such temperature coefficient of $\langle \Delta E \rangle$ would be far from that found for related reactions being analyzed in the same way. It is also at variance with the

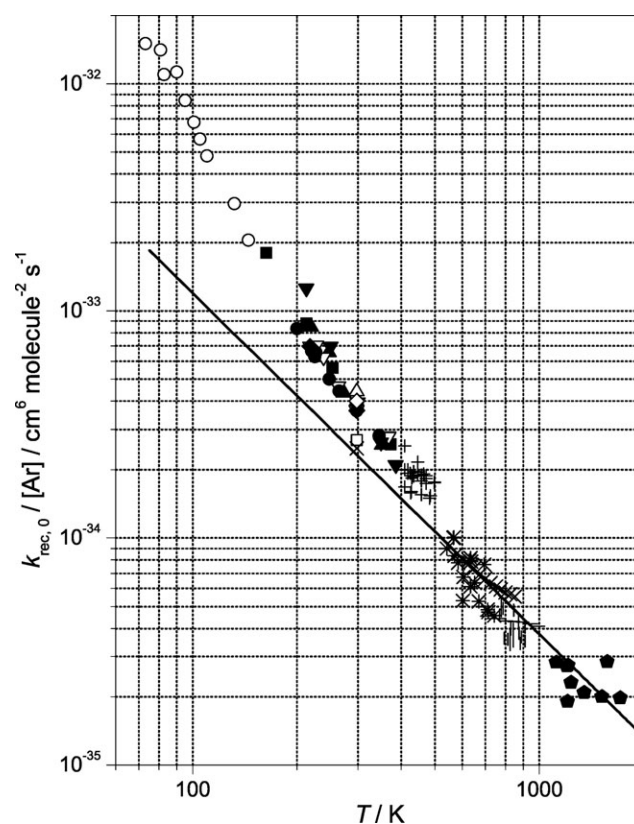


Fig. 1 Low-pressure rate coefficients for ozone recombination in $\text{M} = \text{Ar}$ (experimental points: (○) ref. 10, (■) ref. 11, (▲) ref. 47, (▽) ref. 46, (◆) ref. 45, (□) ref. 42, (●) ref. 41, (△) ref. 40, (▼) ref. 39, (◇) ref. 37, (+) ref. 38, (×) ref. 36, (☆) ref. 48, (*) ref. 44, (–) ref. 7, (●) ref. 43, (l) ref. 35; full line: modelling of $k_{\text{rec},0}^{\text{ET}}$ for the ET-mechanism with $-\langle \Delta E \rangle/hc = 18 \text{ cm}^{-1}$, see text).

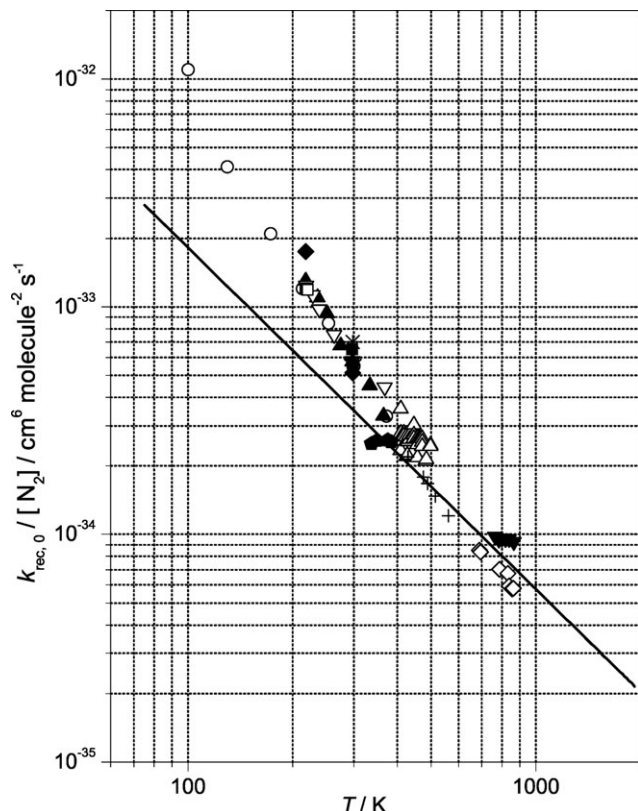


Fig. 2 Low-pressure rate coefficients for ozone recombination in $M = N_2$ (experimental points: (■) ref. 12, (○) ref. 11, (▲) ref. 47, (▽) ref. 46, (◆) ref. 45, (□) ref. 41, (▲) ref. 52, (×) ref. 40, (*) ref. 37, (△) ref. 38, (▼) ref. 7, (◇) ref. 35, (●) ref. 51, (+) ref. 50; full line: modelling of $k_{\text{rec},0}^{\text{ET}}$ for the ET-mechanism with $-\langle\Delta E\rangle/hc = 25 \text{ cm}^{-1}$, see text).

general trends of temperature dependence from directly measured or trajectory calculated $\langle\Delta E\rangle$ at related conditions in various systems.⁴⁹ Therefore, the interpretation of the low temperature data by the ET-mechanism alone can practically be ruled out.

The data base for $M = N_2$ is similarly complete as for $M = \text{Ar}$. Fig. 2 summarizes data from refs. 7, 11, 12, 35, 37, 38, 40, 41, 45, 47, 50–52. In this case we obtain

$$k_{\text{rec},0}^{\text{RC}}/[N_2] = 2.5 \times 10^{-34} (T/300)^{-3.3} \text{ cm}^6 \text{ molecule}^{-2} \text{ s}^{-1} \quad (15)$$

and

$$k_{\text{rec},0}^{\text{ET}}/[N_2] = 3.5 \times 10^{-34} (T/300)^{-1.5} \text{ cm}^6 \text{ molecule}^{-2} \text{ s}^{-1}. \quad (16)$$

The results look similar as for $M = \text{Ar}$. However, both $k_{\text{rec},0}^{\text{ET}}$ and $k_{\text{rec},0}^{\text{RC}}$ are about a factor of 1.5 larger than for $M = \text{Ar}$. An interpretation by the ET-mechanism alone would require $-\langle\Delta E\rangle/hc \approx 70 (T/300)^{-1} \text{ cm}^{-1}$. The value of 70 cm^{-1} would not be much different from the value of 100 cm^{-1} (which corresponds to down step sizes near 200 cm^{-1} at 300 K) which was used in ref. 17. However, as for $M = \text{Ar}$, the temperature coefficient of $\langle\Delta E\rangle$ would be very unusual and different from related reactions analyzed in the same way, as well as from the typical trends in direct determinations of $\langle\Delta E\rangle$ at chemically significant energies.

The picture for $M = \text{He}$ looks slightly different. Fig. 3 summarizes experimental results from refs. 7, 11, 37–39, 41, 47 and 53. The representation shows a curvature which appears to be outside the experimental error. In part, this may be attributed to the positive temperature coefficients of $\langle\Delta E\rangle \propto T^{+0.5}$ used in our analysis which would lead to

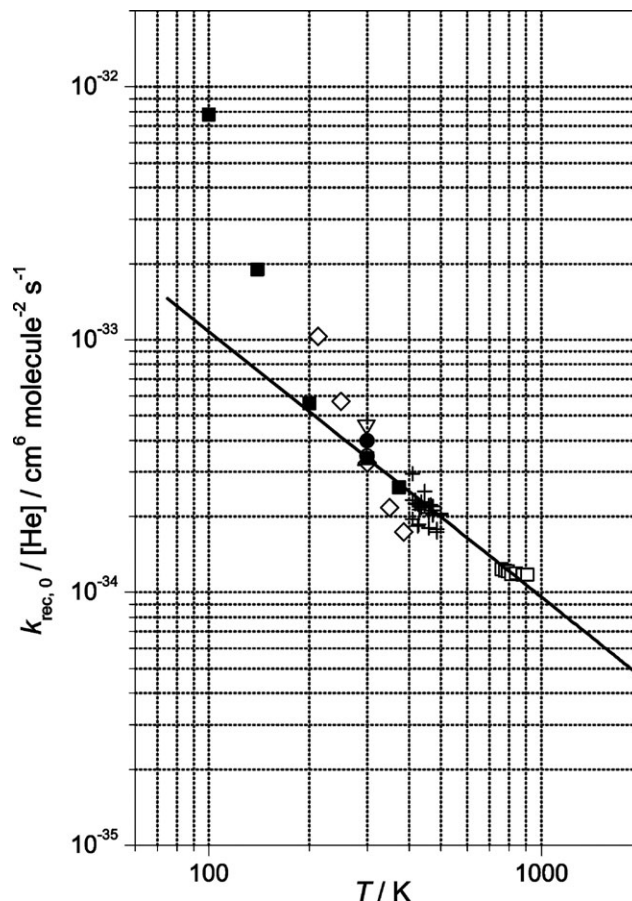


Fig. 3 Low-pressure rate coefficients for ozone recombination in $M = \text{He}$ (experimental points: (■) ref. 11, (○) ref. 47, (△) ref. 41, (▽) ref. 53, (◇) ref. 39, (●) ref. 37, (+) ref. 38, (□) ref. 7; full line: modelling of $k_{\text{rec},0}^{\text{ET}}$ for the ET-mechanism with $-\langle\Delta E\rangle/hc = 18 (T/300)^{0.5} \text{ cm}^{-1}$, see text).

$$k_{\text{rec},0}^{\text{ET}}/[\text{He}] = 3.4 \times 10^{-34} (T/300)^{-1.05} \text{ cm}^6 \text{ molecule}^{-2} \text{ s}^{-1}. \quad (17)$$

However, the data base is too limited at the low and high temperature ends to be sure of the curvature. If eqn. (17) would be adequate, one would have

$$k_{\text{rec},0}^{\text{RC}}/[\text{He}] = 7 \times 10^{-33} \text{ cm}^6 \text{ molecule}^{-2} \text{ s}^{-1} \quad (18)$$

at 100 K and an only negligible contribution from the RC-mechanism at 300 K. If one would assume $\langle\Delta E\rangle \propto T^0$, a smaller value for $k_{\text{rec},0}^{\text{RC}}$ would be derived.

The data base is even less complete for $M = \text{CO}_2$ and SF_6 , see Fig. 4 which compares the data from refs. 7, 36, 37, 39, 42, 54 and 55 for $M = \text{CO}_2$ and from refs. 7, 37 and 42 for $M = \text{SF}_6$. Like for $M = \text{He}$, it would be difficult to separate the contributions from the ET- and RC-mechanisms. However, if the data near 800 K are attributed to the ET-mechanism, one has

$$k_{\text{rec},0}^{\text{ET}}/[\text{CO}_2] = 1.4 \times 10^{-33} (T/300)^{-1.34} \text{ cm}^6 \text{ molecule}^{-2} \text{ s}^{-1} \quad (19)$$

and

$$k_{\text{rec},0}^{\text{ET}}/[\text{SF}_6] = 2.1 \times 10^{-33} (T/300)^{-1.26} \text{ cm}^6 \text{ molecule}^{-2} \text{ s}^{-1}. \quad (20)$$

Through eqn. (12) then

$$k_{\text{rec},0}^{\text{RC}}/[\text{CO}_2] \approx 1 \times 10^{-33} \text{ cm}^6 \text{ molecule}^{-2} \text{ s}^{-1} \quad (21)$$

für $T = 200 \text{ K}$ and

$$k_{\text{rec},0}^{\text{RC}}/[\text{SF}_6] \approx 1 \times 10^{-33} \text{ cm}^6 \text{ molecule}^{-2} \text{ s}^{-1} \quad (22)$$

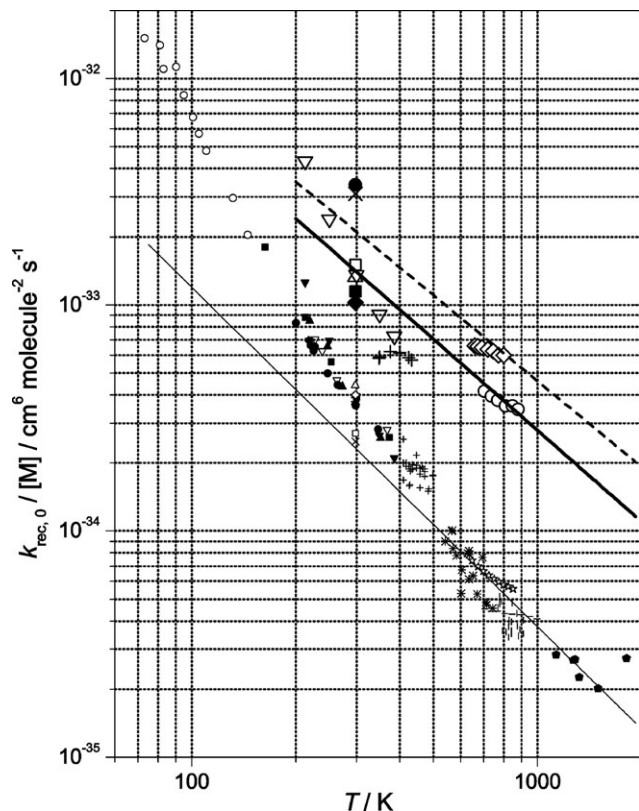


Fig. 4 Low-pressure rate coefficients for ozone recombination in $M = \text{CO}_2$ and SF_6 in comparison to $M = \text{Ar}$ (small symbols with smaller $k_{\text{rec},0}$) (experimental points for $M = \text{CO}_2$: (+) ref. 55, (○) ref. 7, (Δ) ref. 42, (▽) ref. 39, (◆) ref. 54, (□) ref. 37, (■) ref. 36; for $M = \text{SF}_6$: (●) ref. 37, (×) ref. 42, (◇) ref. 7; lines: modelling of $k_{\text{rec},0}^{\text{ET}}$ for the ET-mechanism with $-\langle \Delta E \rangle / hc = 18 \text{ cm}^{-1}$ for $M = \text{Ar}$ (light full line), 150 cm^{-1} for $M = \text{CO}_2$ (heavy full line) and 280 cm^{-1} for $M = \text{SF}_6$ (dashed line), see text).

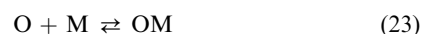
for $T = 300 \text{ K}$ would be estimated; however, these data would be fairly uncertain.

It should be emphasized that the data base for $M = \text{He}$, CO_2 and SF_6 is too small to arrive at a satisfactory separation of the ET- and RC-contributions. However, the data for $M = \text{Ar}$ and N_2 appear sufficient for the separation. An interpretation of the data by the ET-mechanism alone would only be possible with quite unrealistic temperature dependences of $\langle \Delta E \rangle$ such as they have not been found before in this type of analysis. In addition the derived absolute values of $\langle \Delta E \rangle$ would be much larger than have been obtained from classical trajectory calculations of energy transfer of excited ozone, or directly measured in other systems at related conditions.

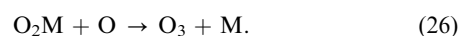
4 Interpretation of the radical complex contribution to the reaction rate

Having empirically determined the contributions $k_{\text{rec},0}^{\text{RC}}$ of the RC-mechanism to the overall rate coefficients $k_{\text{rec},0} = k_{\text{rec},0}^{\text{ET}} + k_{\text{rec},0}^{\text{RC}}$ in the previous section, in the following we try to rationalize the obtained data. The RC-mechanism symbolically

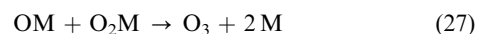
is described by the van der Waals-type equilibria



with the equilibrium constants $K_{23} = ([\text{OM}]/[\text{O}][\text{M}])_{\text{eq}}$ and $K_{24} = ([\text{O}_2\text{M}]/[\text{O}_2][\text{M}])_{\text{eq}}$ and the reactions



In the low-pressure range considered here, reactions of the type



are neglected. Assuming that the pre-equilibria (23) and (24) are established, $k_{\text{rec},0}^{\text{RC}}$ follows as

$$k_{\text{rec},0}^{\text{RC}}/[\text{M}] = k_{25}K_{23} + k_{26}K_{24} \quad (28)$$

The equilibrium constants K_{23} and K_{24} are estimated by a modification of the Bunker-Davidson relationship⁵⁶ such as given by Schwarzer and Teubner.⁵⁷ As the latter authors pointed out, Bunker and Davidson omitted metastable states of the complexes with energies larger than the dissociation energy but smaller than the centrifugal barriers. Including these states increases the equilibrium constants up to a factor of 2 at higher temperatures. Following this method, the equilibrium constants from Table 2 were obtained on the basis of the following Lennard-Jones parameters: $\sigma_{\text{LJ}} = 3.2, 3.5, 3.4, 3.7$ and 4.3 Å and $\varepsilon_{\text{LJ}}/k = 27, 93, 107, 121$ and 126 K for O-He , $-\text{Ar}$, $-\text{N}_2$, $-\text{CO}_2$ and $-\text{SF}_6$ complexes, respectively; $\sigma_{\text{LJ}} = 3.4, 3.6, 3.7$ and 4.3 Å and $\varepsilon_{\text{LJ}}/k = 29, 130, 126, 142$ and 148 K for $\text{O}_2\text{-He}$, $-\text{Ar}$, $-\text{N}_2$, $-\text{CO}_2$ and $-\text{SF}_6$ complexes, respectively, which were taken from refs. 58–60. Assuming $k_{25} \approx k_{26}$, the experiments for $M = \text{Ar}$ and N_2 through eqns. (13), (15) and (28) lead to

$$k_{25} \approx k_{26} \approx 1.2 \times 10^{-12} (T/300)^{-1.4} \text{ cm}^3 \text{ molecule}^{-1} \text{ s}^{-1} \quad (29)$$

for $M = \text{Ar}$ and

$$k_{25} \approx k_{26} \approx 1.1 \times 10^{-12} (T/300)^{-1.7} \text{ cm}^3 \text{ molecule}^{-1} \text{ s}^{-1} \quad (30)$$

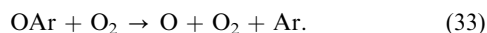
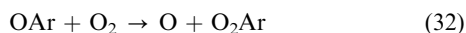
for $M = \text{N}_2$. Following the analysis given, these two values appear now to be established with reasonable certainty. This is much less the case for the results with $M = \text{He}$, CO_2 and SF_6 , see eqns. (18), (21) and (22). Employing the tentative values for the latter bath gases we would obtain $k_{25} \approx k_{26} \approx 8 \times 10^{-11} \text{ cm}^3 \text{ molecule}^{-1} \text{ s}^{-1}$ at 100 K for $M = \text{He}$, $3.8 \times 10^{-12} \text{ cm}^3 \text{ molecule}^{-1} \text{ s}^{-1}$ at 300 K for $M = \text{CO}_2$ and $2.2 \times 10^{-12} \text{ cm}^3 \text{ molecule}^{-1} \text{ s}^{-1}$ at 300 K for $M = \text{SF}_6$. While the latter data, within the uncertainties of our approach appear not unrealistic, clearly the He data are problematic. It appears too difficult to establish $k_{\text{rec},0}^{\text{RC}}$ from few low temperature points only, see Fig. 3, and on the basis of an uncertain temperature dependence of $\langle \Delta E \rangle$. We, therefore, cannot provide a meaningful separation of the He results into ET- and RC-contributions.

In the following we discuss whether the results from eqns. (29) and (30) for $M = \text{Ar}$ and N_2 can be understood in terms of

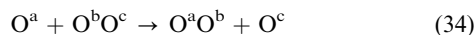
Table 2 Parameters for analyzing $k_{\text{rec},0}^{\text{RC}}$ (K_{23} and K_{24} in $\text{cm}^3 \text{ molecule}^{-1}$, $k_{\text{rec},0}^{\text{RC}}/[\text{M}]$ ($K_{23}+K_{24}$) in $\text{cm}^3 \text{ molecule}^{-1} \text{ s}^{-1}$, $k_{\text{rec},0}^{\text{RC}}/[\text{M}]$ and $k_{\text{rec},0}^{\text{ET}}/[\text{M}]$ in $\text{cm}^6 \text{ molecule}^{-2} \text{ s}^{-1}$; for details, see text)

M	K_{23}	K_{24}	$k_{\text{rec},0}^{\text{RC}}/[\text{M}]$	$k_{\text{rec},0}^{\text{RC}}/[\text{M}]$ ($K_{23} + K_{24}$)	$k_{\text{rec},0}^{\text{ET}}/[\text{M}]$
He	$0.73 \times 10^{-23} (T/300)^{-1.5}$	$1.0 \times 10^{-23} (T/300)^{-1.5}$	—	—	$\approx 3.4 \times 10^{-34} (T/300)^{-1.1}$
Ar	$6.8 \times 10^{-23} (T/300)^{-1.6}$	$12 \times 10^{-23} (T/300)^{-1.6}$	$1.7 \times 10^{-34} (T/300)^{-3.2}$	$1.2 \times 10^{-12} (T/300)^{-1.4}$	$2.3 \times 10^{-34} (T/300)^{-1.5}$
N_2	$7.6 \times 10^{-23} (T/300)^{-1.6}$	$12 \times 10^{-23} (T/300)^{-1.6}$	$2.5 \times 10^{-34} (T/300)^{-3.3}$	$1.3 \times 10^{-12} (T/300)^{-1.7}$	$3.5 \times 10^{-34} (T/300)^{-1.5}$
CO_2	$11 \times 10^{-23} (T/300)^{-1.6}$	$15 \times 10^{-23} (T/300)^{-1.6}$	$\approx 1 \times 10^{-33} (300 \text{ K})$	$\approx 3.8 \times 10^{-12} (300 \text{ K})$	$\approx 10 \times 10^{-34} (T/300)^{-1.4}$
SF_6	$20 \times 10^{-23} (T/300)^{-1.6}$	$26 \times 10^{-23} (T/300)^{-1.6}$	$\approx 1 \times 10^{-33} (300 \text{ K})$	$\approx 2.2 \times 10^{-12} (300 \text{ K})$	$\approx 22 \times 10^{-34} (T/300)^{-1.4}$

related quantities. We consider reaction (25) with $M = \text{Ar}$ as an example. On the one hand this process may be part of a set of competing processes like



On the other hand, it is related to oxygen isotope exchange processes



for which

$$k_{32} \approx (2-3) \times 10^{-12} (T/300)^{-1} \text{ cm}^3 \text{ molecule}^{-1} \text{ s}^{-1} \quad (35)$$

was determined experimentally and analyzed theoretically in refs. 25, 61 and 62. At this stage we note the similarity of the values from eqns. (29), (30) and (35). The slightly different temperature coefficients may attributed to the fact that reaction (33) will become more important than reaction (31) with increasing temperatures and that reaction (34) is closer to reaction (32) than to reaction (31). It also appears not improbable that reaction (31) at room temperature is slower than reaction (34). In any case, the similarity of eqns. (29) and (30) with eqn. (35) in our view presents strong evidence for the validity of the present interpretation.

5 Conclusions

We have reconsidered the experimental data base for ozone recombination and dissociation in the low-pressure limiting range. Assuming that the energy transfer mechanism dominates the reaction at temperatures near 800 K and that the corresponding rate coefficients can safely be extrapolated to lower temperatures, we interpret the differences between measured rate coefficients at lower temperatures and the extrapolations from the ET-mechanism as being due to a contribution from the radical complex mechanism. The derived rate coefficients from the RC-mechanism can well be interpreted in terms of equilibrium constants of O- and O₂-van der Waals complexes and rate coefficients for oxygen abstraction from these complexes. The latter values are very close to rate coefficients for oxygen isotope exchange. This observation strongly supports the present interpretation. A final proof will come from a detailed theoretical modelling of processes of the type of $\text{OAr} + \text{O}_2 \rightarrow \text{O}_3 + \text{Ar}$. Such modelling is underway²⁷ and the preliminary results apparently confirm the present empirically determined values from eqns. (29) and (30).

The present conclusions have also consequences for the interpretation of the isotope effects in ozone recombination which together with the recombination rate is of great importance for atmospheric chemistry. While the ET- and RC-contributions ($k_{\text{rec},0}^{\text{ET}}$ and $k_{\text{rec},0}^{\text{RC}}$, respectively) to the low-pressure rate coefficients $k_{\text{rec},0}$ are of similar magnitude at 300 K with decreasing temperature $k_{\text{rec},0}^{\text{RC}}$ starts to dominate over $k_{\text{rec},0}^{\text{ET}}$. Explanations for the experimentally observed isotope effects, therefore, have to be searched both in the ET- and in the RC-mechanism. The latter to our knowledge has not yet been done. For this reason, we think that the explanation of the isotope effects in ozone recombination still remains an open problem.

Appendix

Molecular parameters for the low-pressure rate coefficients in the ET-mechanism, eqns. (7)–(11)

Lennard-Jones collision parameters. $\sigma_{\text{LJ}}/\text{\AA} = 3.98$ (O₃), 2.551 (He), 3.542 (Ar), 3.798 (N₂), 3.941 (CO₂), 5.128 (SF₆); (ϵ_{LJ}/k)/K = 161.2 (O₃), 10.22 (He), 93.3 (Ar), 71.4 (N₂), 195.2 (CO₂),

Table 3 Numbers of vibrational states of O₃, see text

$(E/hc)/\text{cm}^{-1}$	0	2000	4000	6000	7000	8000	8500
$W_a(E)$	1	7	33	94	143	204	240
$W_b(E)$	1	7	35	100	154	237	303
$W_c(E)$	1	7	33	94	144	179	180

222.1 (SF₆). Fitted average energies transferred per collision $\langle \Delta E \rangle$, see section 2.

Bond energy. $\Delta H_0^\circ = E_0(J=0) = hc\,8475.5 \text{ cm}^{-1}$.⁴⁻⁶

Rotational constants. O₃: 3.553 81, 0.445 30, 0.394 77 cm^{-1} ; O₂: 1.437 66 cm^{-1} .⁶

Electronic states. O₃: $g = 1$; O₂: $g = 3$; O: 0 ($g = 5$), 158.265 ($g = 3$), 226.977 ($g = 1$) cm^{-1} .⁶

Fundamental frequencies. O₃: 1103, 701, 1042 cm^{-1} ;⁶³ O₂: 1556 cm^{-1} .⁶

Anharmonic vibrational densities of states. Spectroscopic constants for O₃: $\omega_1 = 1134.3$, $\omega_2 = 713.5$, $\omega_3 = 1097.4$, $x_{11} = -6.89$, $x_{22} = -1.28$, $x_{33} = -10.94$, $x_{12} = -8.25$, $x_{13} = -36.83$, $x_{23} = -17.62$;⁶⁴ anharmonic numbers of vibrational states $W(E)$ are determined with the spectroscopic constants ($W_a(E)$) or with the empirical anharmonicity model from ref. 65 ($W_b(E)$), the harmonized frequencies 1201.99, 724.28, 1058.98 cm^{-1} and local bond energies 9114.4, 42044 cm^{-1} reproduce the fundamental frequencies, see ref. 65). They are compared with the accurate values ($W_c(E)$) from an *ab initio* potential.²² Table 3 shows the results ($E = \text{energy}$ above the vibrational ground state of O₃).

Because of the sparsity of levels, densities of states $\rho_{\text{vib}}(E) = dW(E)/dE$ have to be smoothed. The Whitten–Rabinovitch expression⁶³ gives $\rho_{\text{vib},h}(E_0) = 0.061/\text{cm}^{-1}$ employing fundamental frequencies and the Whitten–Rabinovitch parameter $a(E_0) = 0.984$. One obtains $dW_a(E)/dE \approx 0.065/\text{cm}^{-1}$, $dW_b(E)/dE \approx 0.082/\text{cm}^{-1}$ and $dW_c(E)/dE \approx 0.07/\text{cm}^{-1}$ at $E = E_0$, see ref. 21. Using the Whitten–Rabinovitch value, such as calculated with the anharmonic fundamental frequencies, for $\rho_{\text{vib},h}(E_0) = 0.061/\text{cm}^{-1}$, with $\rho_{\text{vib}}(E_0) \approx 0.082/\text{cm}^{-1}$ one has $F_{\text{anh}} \approx 1.34$ which is used here; an overestimate of F_{anh} of about 15% appears possible, but would be compensated by lowering β_c and $\langle \Delta E \rangle$ correspondingly.

Centrifugal barriers $E_0(J)$ and rotational factors $F_{\text{rot}}(T)$. Centrifugal barriers are calculated with a fit to the *ab initio* potential from ref. 25 (Fig. 1) as represented by $V(r) = E_0 + D_1\{\exp[-2\beta_1(r - r_{e1})] - 2\exp[-\beta_1(r - r_{e1})]\} - D_2\{\exp[-2\beta_2(r - r_{e2})] - 2\exp[-\beta_2(r - r_{e2})]\}$ with the center-of-mass O–O₂ distance r , $D_1/hc = 409.4 \text{ cm}^{-1}$, $D_2/hc = 230.4 \text{ cm}^{-1}$, $r_{e1} = 2.704 \text{ \AA}$, $r_{e2} = 2.637 \text{ \AA}$, $\beta_1 = 1.987 \text{ \AA}^{-1}$, $\beta_2 = 2.932 \text{ \AA}^{-1}$. Because of the presence of a potential reef 114 cm^{-1} below the dissociation limit²⁵ at c.o.m. distance $r \approx 2.4 \text{ \AA}$, there is centrifugal barrier switching at $J \approx 28$. For $J \leq 28$, one obtains $E_0(J) - E_0(J=0) \approx hc\,9.0 \times 10^{-3} [J(J+1)]^{1.21} \text{ cm}^{-1}$; for $J > 28$, one has $E_0(J) - E_0(J \approx 0) \approx hc\,1.3 \times 10^{-1} [J(J+1)]^{1.36} \text{ cm}^{-1}$. $F_{\text{rot}}(T)$ was calculated with the accurate $E_0(J)$ using the method of ref. 9 and leading to $F_{\text{rot}}(T) = 26.2, 15.4, 11.7, 9.7, 7.4, 6.0, 5.0, 3.5$ in comparison to $F_{\text{rot,max}}(T)$ (see ref. 9) = 292, 103, 56, 37, 20, 13, 9.2, 5.0 for $T/\text{K} = 100, 200, 300, 400, 600, 800, 1000, 1500$. $F_{\text{rot}}(T)$ can well be approximated by $F_{\text{rot}} \approx 11.7(T/300)^{-0.71}$.

Acknowledgements

Financial support of this work by the Deutsche Forschungsgemeinschaft (SFB 357 "Molekulare Mechanismen unimolekularer Prozesse") and Alexander von Humboldt Foundation ("Sofja Kovalevskaja Program") as well as extensive discussions with R. Schinke, V. G. Ushakov, and many other colleagues are gratefully acknowledged.

References

- 1 D. L. Baulch, D. D. Drysdale, J. Duxbury and S. J. Grant, *Evaluated Kinetic Data for High Temperature Reactions*, Butterworth, London, 1976, vol. 3, pp. 65–123.
- 2 D. L. Baulch, R. A. Cox, R. F. Hampson, J. A. Kerr and R. T. Watson, *J. Phys. Chem. Ref. Data*, 1980, **9**, 295.
- 3 D. L. Baulch, R. A. Cox, P. J. Crutzen, R. F. Hampson, J. A. Kerr, J. Troe and R. T. Watson, *J. Phys. Chem. Ref. Data*, 1982, **11**, 327.
- 4 R. Atkinson, D. L. Baulch, R. A. Cox, R. F. Hampson, J. A. Kerr, M. J. Rossi and J. Troe, *J. Phys. Chem. Ref. Data*, 1997, **26**, 1329.
- 5 S. P. Sander, R. R. Friedl, D. M. Golden, M. J. Kurylo, R. E. Huie, V. L. Orkin, G. Moortgat, A. R. Ravishankara, C. E. Kolb, M. J. Molina and B. J. Finlayson-Pitts, *JPL Publ.*, 2003, **02–25**.
- 6 M. W. Chase, "NIST-JANAF Thermochemical Tables", *J. Phys. Chem. Ref. Data*, 4th edn., 1998, Monograph No. 9.
- 7 H. Endo, K. Glänzer and J. Troe, *J. Phys. Chem.*, 1979, **83**, 2083.
- 8 J. Troe, *J. Chem. Phys.*, 1977, **66**, 4758.
- 9 (a) J. Troe, *J. Phys. Chem.*, 1979, **83**, 114; (b) see also: R. Patrick and D. M. Golden, *Int. J. Chem. Kinet.*, 1983, **15**, 1189.
- 10 W. T. Rawlins, G. E. Caledonia and R. A. Armstrong, *J. Chem. Phys.*, 1984, **87**, 5209.
- 11 H. Hippler, R. Rahn and J. Troe, *J. Chem. Phys.*, 1990, **93**, 6560.
- 12 (a) S. Anderson, D. Hülsebusch and K. Mauersberger, *J. Chem. Phys.*, 1997, **107**, 5383; (b) K. Mauersberger, B. Erbacher, D. Krankowsky, J. Günther and R. Nickel, *Science*, 1999, **283**, 370.
- 13 C. Janssen, J. Günther, K. Mauersberger and D. Krankowsky, *Phys. Chem. Chem. Phys.*, 2001, **3**, 4718.
- 14 C. Janssen, J. Guenther, D. Krankowsky and K. Mauersberger, *Chem. Phys. Lett.*, 2003, **367**, 34.
- 15 (a) B. C. Hathorn and R. A. Marcus, *J. Chem. Phys.*, 1994, **111**, 4087; (b) B. C. Hathorn and R. A. Marcus, *J. Chem. Phys.*, 2000, **113**, 9497.
- 16 R. A. Marcus and Y. Q. Gao, *J. Chem. Phys.*, 2001, **114**, 9807.
- 17 (a) Y. Q. Gao and R. A. Marcus, *J. Chem. Phys.*, 2002, **116**, 137; (b) V. Q. Gao, W.-C. Chen and R. A. Marcus, *J. Chem. Phys.*, 2002, **117**, 1536.
- 18 A. Miklavc and S. Peyerimhoff, *Chem. Phys. Lett.*, 2002, **359**, 55.
- 19 (a) D. Charlo and D. C. Clary, *J. Chem. Phys.*, 2002, **117**, 1660; (b) T. A. Baker and G. I. Gellene, *J. Chem. Phys.*, 2002, **117**, 7603; (c) A. Gross and G. D. Billing, *Chem. Phys.*, 1993, **173**, 303; (d) A. Gross and G. D. Billing, *Chem. Phys.*, 1994, **187**, 329.
- 20 A. J. C. Varandas, A. A. C. C. Pais, J. M. C. Marques and W. Wang, *Chem. Phys. Lett.*, 1996, **249**, 264.
- 21 R. Siebert, R. Schinke and M. Bittererová, *Phys. Chem. Chem. Phys.*, 2001, **3**, 1795.
- 22 R. Siebert, P. Fleurat-Lessard, M. Bittererová, S. C. Farantos and R. Schinke, *J. Chem. Phys.*, 2002, **116**, 9742.
- 23 (a) D. Babikov, B. K. Kendrick, R. B. Walker, R. T. Pack, P. Fleurat-Lessard and R. Schinke, *J. Chem. Phys.*, 2003, **118**, 6298; (b) D. Babikov, B. K. Kendrick, R. B. Walker, R. T. Pack, P. Fleurat-Lessard and R. Schinke, *J. Chem. Phys.*, 2003, **119**, 2577.
- 24 K. Luther, K. Oum, K. Sekiguchi and J. Troe, *Phys. Chem. Chem. Phys.*, 2004, **6**, 4133.
- 25 P. Fleurat-Lessard, S. Y. Grebenshchikov, R. Siebert and R. Schinke, *J. Chem. Phys.*, 2003, **118**, 610.
- 26 M. V. Ivanov, S. Yu. Grebenshchikov and R. Schinke, *J. Chem. Phys.*, 2004, **120**, 10015, and work in progress (Göttingen, 2005).
- 27 M. Ivanov and R. Schinke, work in progress (Göttingen, 2005).
- 28 J. Troe, *J. Chem. Phys.*, 1977, **66**, 4745.
- 29 J. Troe, *Annu. Rev. Phys. Chem.*, 1978, **29**, 223.
- 30 A. J. Stace and J. N. Murrell, *J. Chem. Phys.*, 1978, **68**, 3028.
- 31 A. Gelb, *J. Phys. Chem.*, 1985, **89**, 4189.
- 32 J. Troe, *Proc. Combust. Inst.*, 2000, **28**, 1463.
- 33 C. J. Cobos and J. Troe, *Z. Phys. Chem.*, 1992, **176**, 161.
- 34 C. J. Cobos and J. Troe, *Z. Phys. Chem.*, 1990, **167**, 129.
- 35 W. M. Jones and N. Davidson, *J. Am. Chem. Soc.*, 1962, **84**, 2868.
- 36 M. C. Sauer and L. M. Dorfman, *J. Am. Chem. Soc.*, 1965, **87**, 3801.
- 37 F. Kaufman and J. R. Kelso, *J. Chem. Phys.*, 1967, **46**, 4541.
- 38 E. I. Intezarova and V. N. Kondratiev, *Izv. Akad. Nauk. SSSR, Ser. Khim.*, 1967, **11**, 2440, revaluated with $k(\text{O} + \text{O}_3 \rightarrow 2\text{O}_2)$ from ref. 35.
- 39 M. F. R. Mulcahy and D. J. Williams, *Trans. Faraday Soc.*, 1968, **64**, 59 (scaled to $k_{\text{rec},0}$ (300 K) from ref. 37).
- 40 T. G. Slanger and G. Black, *J. Chem. Phys.*, 1970, **53**, 3717.
- 41 R. E. Huie, J. T. Herron and D. D. Davis, *J. Phys. Chem.*, 1972, **76**, 2653.
- 42 P. L. T. Bevan and G. R. A. Johnson, *J. Chem. Soc., Faraday Trans.*, 1973, **69**, 216.
- 43 R. E. Center and R. T. V. Kung, *J. Chem. Phys.*, 1975, **62**, 802 (only data with 1% O_3 in Ar at $T \leq 1500$ K are considered).
- 44 C. Park, *J. Phys. Chem.*, 1977, **81**, 499.
- 45 I. Arnold and F. J. Comes, *Chem. Phys.*, 1979, **42**, 231.
- 46 O. Klais, P. C. Anderson and M. J. Kurylo, *Int. J. Chem. Kinet.*, 1980, **12**, 469.
- 47 C. L. Lin and M. T. Leu, *Int. J. Chem. Kinet.*, 1982, **14**, 417.
- 48 B. S. Lunin, O. V. Kuricheva and Yu. N. Zhitnev, *Russ. J. Phys. Chem.*, 1986, **60**, 2050.
- 49 U. Grigoleit, T. Lenzer and K. Luther, *Z. Phys. Chem.*, 2000, **214**, 1065.
- 50 D. Garvin, *J. Am. Chem. Soc.*, 1954, **76**, 1523.
- 51 S. W. Benson and A. E. Axworthy, *J. Chem. Phys.*, 1957, **26**, 1718.
- 52 F. Stuhl and H. Niki, *J. Chem. Phys.*, 1971, **55**, 3943.
- 53 R. J. Donovan, D. Husain and L. J. Kirsch, *Trans. Faraday Soc.*, 1970, **66**, 2551.
- 54 G. M. Meaburn, D. Perner, J. LeCalve and M. Bourene, *J. Phys. Chem.*, 1968, **72**, 3920.
- 55 S. Toby and E. Ullrich, *Int. J. Chem. Kinet.*, 1980, **12**, 535.
- 56 D. L. Bunker and N. Davidson, *J. Am. Chem. Soc.*, 1958, **80**, 5090.
- 57 D. Schwarzer and M. Teubner, *J. Chem. Phys.*, 2002, **116**, 5680.
- 58 (a) E. Luzzatti, F. Pirani and F. Vecchiocattivi, *Mol. Phys.*, 1977, **34**, 1279; (b) V. Aquilanti, R. Candori, E. Luzzatti, F. Pirani and G. G. Volpi, *J. Chem. Phys.*, 1985, **85**, 5377.
- 59 B. Brunetti, G. Liuti, E. Luzzatti, F. Pirani and F. Vecchiocattivi, *J. Chem. Phys.*, 1981, **74**, 6734.
- 60 H. Hippler, J. Troe and H. J. Wendelken, *J. Chem. Phys.*, 1983, **78**, 6709.
- 61 W. E. Wiegell, N. W. Larsen, T. Pedersen and H. Egsgaard, *Int. J. Chem. Kinet.*, 1997, **29**, 745.
- 62 P. Fleurat-Lessard, S. Y. u. Grebenshchikov, R. Schinke, C. Janssen and D. Krankowsky, *J. Chem. Phys.*, 2003, **119**, 4700.
- 63 A. Barbe, C. Secroun and P. Jouve, *J. Mol. Spectrosc.*, 1974, **49**, 171.
- 64 K. A. Peterson, R. C. Mayrhofer, E. L. Sibert and R. C. Woods, *J. Chem. Phys.*, 1991, **94**, 414.
- 65 J. Troe, *Chem. Phys.*, 1995, **190**, 381.